Journal of *Marine Science and Engineering*

MDPI

Article

Formation Mechanism of NW-Trending Faults and Their Significance on Basin Evolution in Zhu III Depression of the Pearl River Mouth Basin, SE China

Pengfei Zhu [1,2,†], Lintao Zhao [3,4,†], Jiantai Zhang [5], Dunling Mu [1,2,*], Yichun Chen [1,2] and Pengfei Rong [1,2]

1 Institute of Digital Geology and Energy, Linyi University, Linyi 276000, China; zzpf4377zz@163.com (P.Z.); chunzhi233233@hotmail.com (Y.C.); rpf15954643405@163.com (P.R.)
2 Shandong Provincial Key Laboratory of Water and Soil Conservation and Environmental Protection, School of Resource and Environment (College of Carbon Neutrality), Linyi University, Linyi 276000, China
3 Key Laboratory of Tropical Marine Ecosystem and Bioresource, Fourth Institute of Oceanography, Ministry of Natural Resources, Beihai 536000, China; zhaolintao@4io.org.cn
4 Guangxi Key Laboratory of Beibu Gulf Marine Resources, Environment and Sustainable Development, Fourth Institute of Oceanography, Ministry of Natural Resources, Beihai 536000, China
5 The Seventh Geological Brigade of Shandong Provincial Bureau of Geology and Mineral Exploration and Development, Linyi 276000, China; jiantai26@126.com
* Correspondence: 17505324322@163.com
† These authors contributed equally to this work.

Abstract: The Zhu III Depression, situated in the northern Pearl River Mouth Basin, features a complex fault system composed of NE–SW-, nearly E–W-, and NW–SE-oriented faults. However, there is limited research on NW-trending faults, especially regarding their formation mechanisms. Through structural analysis of 3D seismic profiles, we have revealed the geometric and kinematic characteristics of NW-trending faults and categorized them into three types based on their formation mechanisms: extensional fault, dextral transtensional fault, and sinistral strike–slip fault. The extensional faults predominantly developed as boundary faults during the rifting I period, caused by tectonic inversion of the NW–NWW-trending basement faults since early Eocene. The transtensional fault resulted from the dextral strike–slip motion of the NE-trending basin-controlling faults since late Eocene, under the regional dextral extension stress setting. The sinistral strike–slip faults have been dominant during the post-rifting period since early Oligocene. This is due to the sinistral shearing action related to the southeastward lateral extrusion of the Indochina Block and slab pull southward by subduction of the proto-SCS. The NW-trending faults controlled the development of local tectonics and structures, the depocenter migration during the rifting period, and the trapping, migration, and preservation of oil and gas.

Keywords: strike–slip fault; formation mechanism; seismic interpretation; Zhu III Depression; Pearl River Mouth Basin

Citation: Zhu, P.; Zhao, L.; Zhang, J.; Mu, D.; Chen, Y.; Rong, P. Formation Mechanism of NW-Trending Faults and Their Significance on Basin Evolution in Zhu III Depression of the Pearl River Mouth Basin, SE China. *J. Mar. Sci. Eng.* **2024**, *12*, 858. https://doi.org/10.3390/jmse12060858

Academic Editor: Gemma Aiello

Received: 25 April 2024
Revised: 15 May 2024
Accepted: 20 May 2024
Published: 22 May 2024

1. Introduction

Faults are the main deformation style of basin tectonic activity, not only controlling the evolution of the basin, but also serving as the main migration channel for oil and gas in the basin, and further controlling the formation and distribution of oil and gas reservoirs [1–6]. In the Cenozoic, the East Asian Continental Margin developed intense rifting, producing massive rift basins and marginal seas. Among these, the South China Sea (SCS) and adjacent continental margin have attracted attention due to the obscure opening mechanism and strong lithospheric thinning [7–9]. As a representative of the epicontinental rift basin in the northern margin of the South China Sea (NSCS), the Pearl River Mouth Basin (PRMB) is an ideal study area for a better understanding of the tectonic evolution of the South China Block and the time limit of the opening of the SCS. The Zhu III Depression,

a secondary structural unit located in the northwest of the PRMB, is an important region for oil and gas exploration in the west of the SCS. In recent years, extensive research has been conducted on the complex fault system and its relationship with sedimentary evolution and oil–gas distribution in the basin [10–16]. The tectonic units of the Zhu III Depression (even the PRMB) and main faults in the rifting period mostly extend in the NE striking, thus research on the fault system of the Zhu III Depression has mainly focused on the NE-trending faults, while relatively less attention has been paid to the NW–NWW-trending faults. However, there are several large basin-controlling fault zones trending NW, such as the Yangjiang–Yitong Fault. Additionally, some NW-trending secondary faults related to the basement faults are also found in depressions [17–19]. Especially in the post-rifting stage, the NW-trending faults increased and became the dominant faults [20–22], which induced local uplift activity and controlled the trapping, migration, and preservation of oil and gas [23,24]. It is thus clear that the NW-trending fault is very important for the evolution of the basin. However, there are still differing views on the formation mechanisms of NW-trending faults, including extension and strike–slip motion [25–27].

A detailed study of faults is crucial for understanding the process of tectonic evolution and the dynamic mechanisms of the basin, revealing patterns of hydrocarbon accumulation and guiding the implementation of oil and gas exploration. The continuous acquisition of 3D seismic and well data by the China National Offshore Oil Corporation (CNOOC) Shenzhen Branch and associated cooperative services companies over the past decades has provided a sufficient basis for our research. Therefore, building on previous studies, this paper conducts a detailed interpretation and analysis of the NW-trending (including NWW-trending) faults in the Zhu III Depression using 3D seismic data. Our aim is to reveal the geometric and kinematic characteristics of the faults, discuss their formation mechanisms, and explore their impact on the tectonic evolution of the basin and hydrocarbon accumulation. This study will provide reference for the formation mechanism of the rifting basins in the northern continental margin of the South China Sea.

2. Geological Setting

The South China Sea (SCS) is at the convergence of the Pacific Plate (Philippines Sea Plate), the Indo–Australian Plate, and the Eurasian Plate. It records the interaction among multiple surrounding plates and has been considered a natural laboratory for studying the tectonic evolution of marginal seas [28–32]. However, the origin of the SCS remains obscure, and four principal tectonic models have been proposed for SCS opening: (1) slab pull from subduction of a proto-South China Sea; (2) extrusion tectonics from the India–Asia collision; (3) basal drag from a mantle plume; and (4) backarc rifting [33–38]. The PRMB (Figure 1a) located on the NSCS is a Cenozoic petroliferous basin developed above the Mesozoic tectonic basement [18,39]. Previous studies have revealed that the Mesozoic basement structure of the PRMB is mainly controlled by a NE- and NW-trending conjugate fault system [40–42]. During the Cenozoic, the basin experienced a rifting period in Paleocene–early Oligocene and a depression period since late Oligocene (Figure 2). The rifting of the basin is controlled by the Zhu–Qiong Movement. The first episode of the Zhu–Qiong Movement occurred in the Early to Middle Eocene, corresponding to the seismic reflection interface T90, which is the bottom interface of the Wenchang Formation. The seismic wave features above the interface are distinctly stratified, while those below are more chaotic, representing the beginning of large-scale rifting and faulting. The second episode of the Zhu–Qiong Movement is a significant tectonic event that occurred in the Late Eocene, represented on the seismic profile as the T80 unconformity, which is the bottom interface of the Enping Formation. This event, distinguished from the first episode of the Zhu–Qiong Movement, caused regional uplift in the basin, accompanied by faulting and magmatic activity, although it has been considered a continuation of the first episode. Thus, the rifting period has been further divided into the rifting I period and the rifting II period, with the T80 interface as the boundary [43,44]. In addition, the Transition and Neotectonic period can be classified as the post-rifting thermal subsidence period (depression) [45,46].

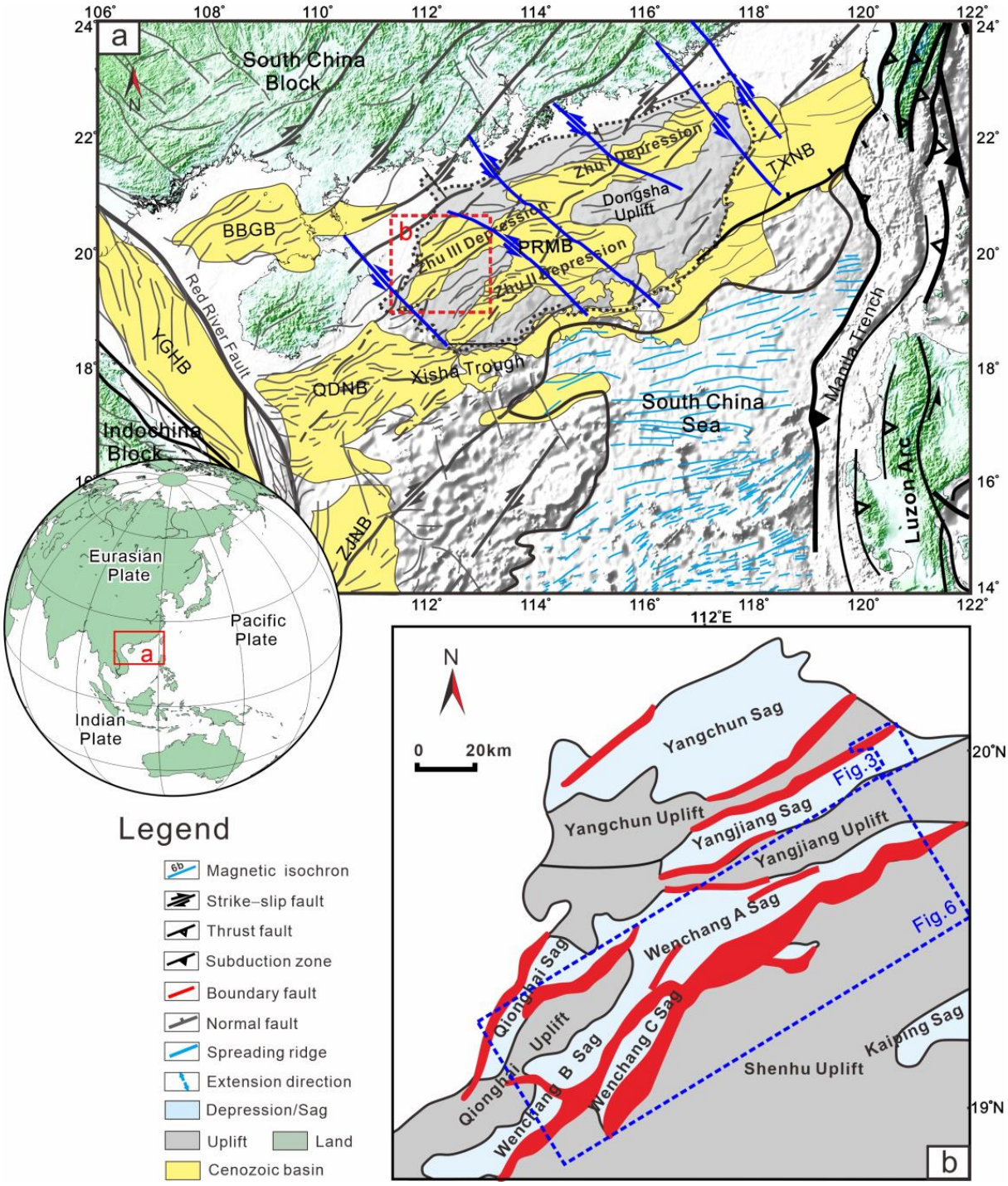

Figure 1. Regional structural map of PRMB (**a**) and the distribution of structural units and fault system of Zhu III Depression (**b**). The schematic diagram in the lower left shows the location of the PRMB and the NSCS. The fault pattern is modified after [8,47]. The magnetic isochrons are adopted from [48]. BBGB: Beibu Gulf Basin; QDNB: Qiongdongnan Basin; PRMB: Pearl River Mouth Basin; TXNB: Taixinan Basin; YGHB: Yinggehai Basin; ZJNB: Zhongjiannan Basin.

As a result, a tectonic framework characterized by lower faulting and upper depression has been established. From north to south, the basin can be divided into five first-order structural units: the northern uplift zone, the northern depression zone, the central uplift zone, the southern depression zone, and the southern uplift zone (Figure 1a).

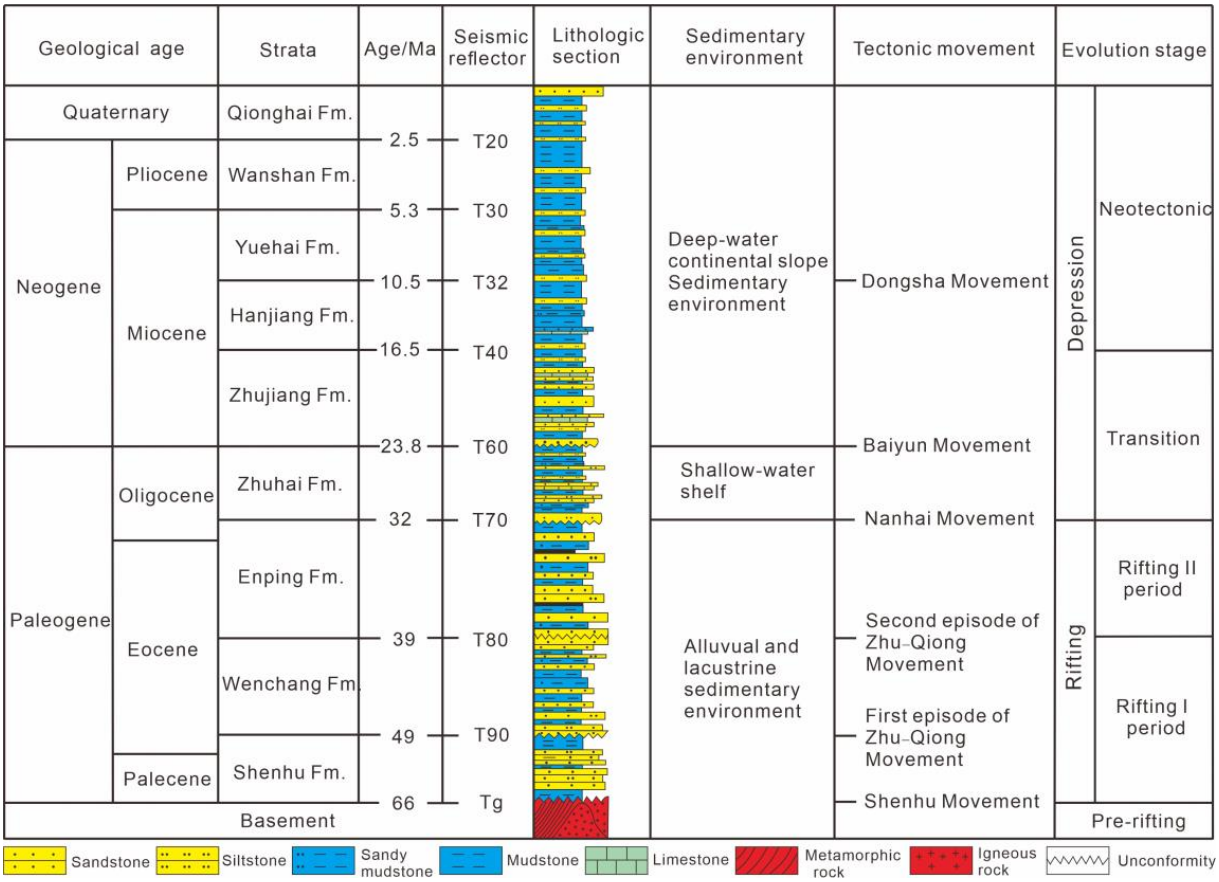

Figure 2. Comprehensive sequence columns of the PRMB [2,21].

The Zhu III Depression is a secondary structural unit in the west of the northern depression zone. It is separated from the Zhu I Depression by the Yangjiang–Yitong fault zone to the east and is adjacent to the Shenhu uplift to the south. From north to south, the Zhu III Depression is composed of the Yangchun Sag, Yangchun Uplift, Yangjiang Sag, Yangjiang Uplift, Qionghai Sag, Qionghai Uplift, and Wenchang Sag. These secondary structural units mainly appear in a NE direction, characterized in belt distribution (Figure 1b). From bottom to top, the sedimentary strata developed in the depression include the Paleogene Shenhu Formation, Wenchang Formation, Enping Formation, Zhuhai Formation, Neogene Zhujiang Formation, Hanjiang Formation, Yuehai Formation, Wanshan Formation, and Quaternary Qionghai Formation (Figure 2). Exploration practices have revealed that the Yangjiang Sag and Wenchang Sag are significant hydrocarbon-generating sags in the Zhu III Depression, and two sets of important hydrocarbon source rocks are developed in the Paleogene Wenchang and Enping Formation [24,49,50].

The Zhu III Depression features a complex fault system containing NE-, nearly E–W-, and NW-striking faults. It is revealed that the formation of multi-striking faults is closely related to both the pre-existing basement structures and the continuous dextral variation of the regional extensional tectonic stress field since the Cenozoic [19,42,51,52]. There is a basin-controlling fault zone trending NW in the east of the Zhu III Depression called the Yangjiang–Yitong fault zone. The northern segment of the fault zone separates the Zhu III and Zhu I depressions and was active from Mesozoic to Cenozoic, which has a great impact on the development of the Zhu III Depression [41,53], especially for the adjacent Yangjiang Sag [27,54]. Additionally, a NE-striking depression-controlling fault, known as the Zhu III South Fault, governed the formation of the Zhu III Depression as a half-graben, with faulting in the south and overlapping in the north. Given the development of en echelon folds, horsetail faults, and oblique steps in the Wenchang Sag, it is revealed that the

Zhu III South Fault has undergone dextral strike–slip deformation [10,15,25,26,32]. Except the boundary fault, it has also been revealed that strike–slip activity occurred along the faults within the depression. Based on the tectonic analysis of the Wenchang Sag, the fault system is further categorized into early NE-trending extensional faults, middle E–W-trending extensional–dextral strike–slip faults, and late NW-trending extensional–sinistral strike–slip faults [11,55]. Structure studies show that after the initial rifting, the Yangjiang Sag successively experienced two stages of strike–slip pull apart movement in NE and NW directions, respectively [8,21,54,56]. This provides a basis for establishing the strike–slip model for basin formation rather than a single extension model.

3. Data and Methods

The 3D seismic and well data used in our fault interpretation were provided by the China National Offshore Oil Corporation (CNOOC) Shenzhen Branch and associated cooperative service companies. The seismic profiles utilized in this study offer comprehensive coverage of the Yangjiang Sag, spanning an area of over 5600 km^2. The bin size of the survey is 12.5 m × 12.5 m. The inline seismic profiles are oriented NW, which is approximately perpendicular to the trend of the basin. We adhered to standard seismic interpretation workflows for tectonic–stratigraphic analysis and identification of magmatic bodies,. We established a robust stratigraphic framework by integrating 3D seismic and log data with vertical seismic profile (VSP) information from select typical wells. Exploration wells from the Yangjiang Sag and Enping Sag have also been utilized for depth conversion by (1). Given the relatively complete stratigraphic sequence, petroleum exploration boreholes served as a calibration tool for the Cenozoic strata. This approach ensures that our interpretations are rooted in well–understood geological structures and sequences, thereby enhancing the reliability and validity of our findings.

$$D = 0.00027451t2 + 0.72410996t + 31.78776360,\ R2 = 0.99991635 \quad (1)$$

where D represents the depth, t represents the time, and R2 represents the goodness of fit.

We employed traditional manual interpretation of the 3D seismic data to unveil the geometric shape, combination style, and distribution pattern of faults in plan-section views. This was further validated and constrained using methods such as coherence analysis of the 3D seismic data. Our workflow comprised the following steps: (1) identification and correlation of seismic horizons; (2) generation of time structural maps, seismic volume slices, and fault distribution maps during the different seismic reflectors; (3) observation of strike–slip structures; (4) investigation of changes of depocenters; (5) calculation of fault activity rates; (6) analysis of the mechanism and dynamic process of fault formation; (7) exploration of the significance of faults on basin evolution. Among them, the interpretation of strike–slip faults is relatively difficult. Based on previous research [57,58], we mainly applied the following approaches for identification: (1) determination of fault location based on seismic attributes. We analyzed seismic wavegroup characteristics, maximum amplitude attributes, and data volume slices to identify fault locations. (2) Identification of strike–slip structures based on fault combination relationships. This was comprehensively identified from two aspects: plan and section views. (a) On the plan view, we focused on linearly extended or band-distributed structures, pull-apart structures, en echelon faults or en echelon folds, horsetail structures, plumosestructures, and horizontal offset of geological boundaries on both sides of the faults. (b) On the section view, based on the fault surface attitude (steep and penetrating the basement), we identified flower-like structures, “ribbon effect”, “dolphin effect”, and discordance in the thickness, sedimentary facies, and stratum attitude of the same stratigraphic unit on both sides of the fault.

4. Results

4.1. Fault Patterns of the Yangjiang Sag

The Yangjiang Sag is located in the east of the Zhu III Depression, with the Yangjiang–Yitong fault zone crossing its eastern part. NW-trending faults have developed in the Yangjiang Sag, even though the fault system was dominated by NE-direction faults during the rifting I period during early–middle Eocene (Figure 3). In the east Yangjiang Sag, the F20 fault with a westward-dipping fault surface and the F19 fault with an east-dipping fault surface were formed trending NNW, becoming important boundary faults in the east and west of the Enping 20 subsag. The two faults cut the Wenchang Formation with significant fault throws at about 800 m, and there are obvious differences in strata thickness between the two sides of the fault. Therefore, they were synsedimentary faults and controlled the deposition of Wenchang Formation. Contemporaneously, the NWW-trending, south-dipping, sag-controlling F7 fault also formed, of which the maximum dip–slip active rate has reached 130 m/Ma (Figure 4b), which controlled the intense initial rifting process of the Enping 27 subsag. Additionally, some secondary faults, trending NW–NWW and mostly curved in shape, have formed within the Yangjiang Sag. These faults are relatively small in size with short lengths. These faults have partially influenced the control of rifting and sedimentation.

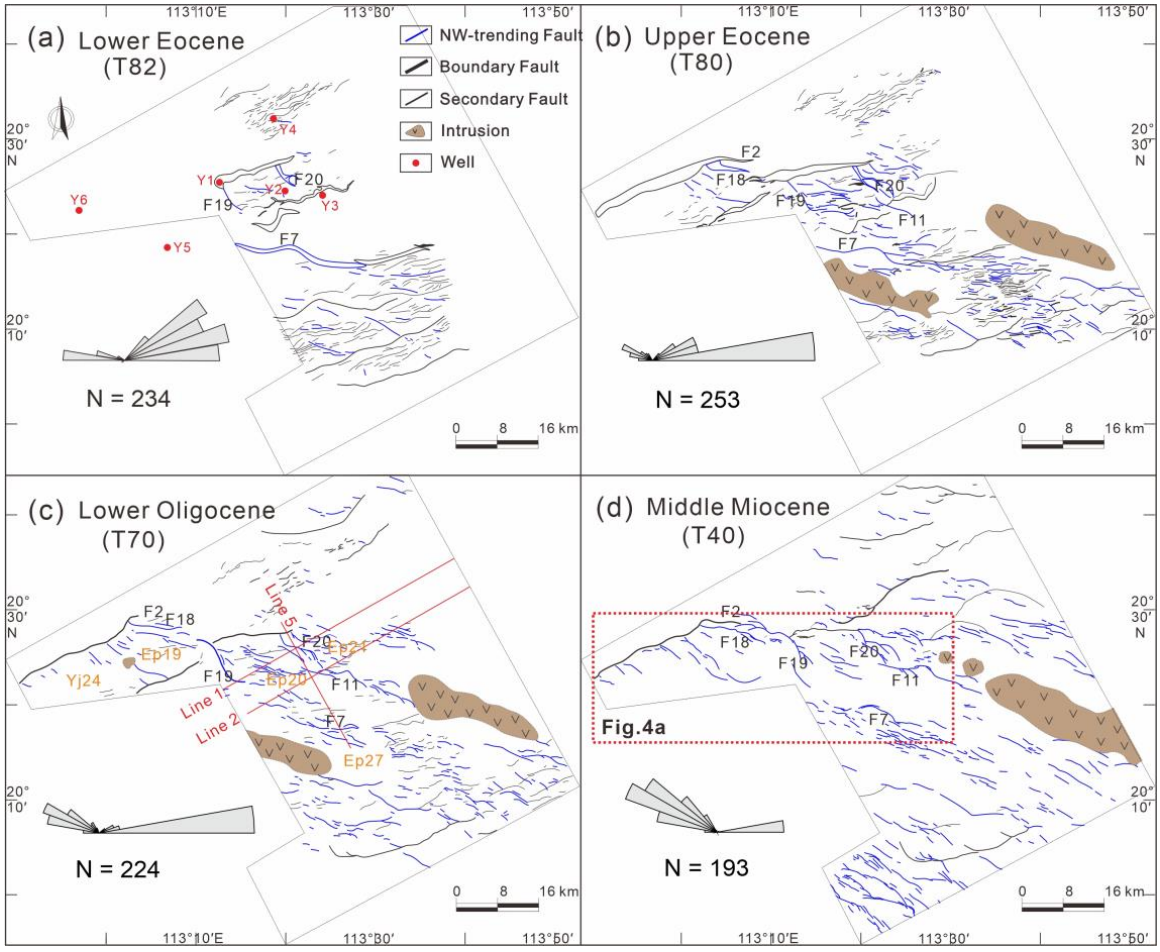

Figure 3. Fault patterns and rose diagram in different seismic reflectors of the Yangjiang Sag. The rose diagram shows stripes and strikes of the faults in seismic reflectors. The faults were drawn using more than 100 seismic lines for the Yangjiang Sag, and the strike data of the fault are from [27]. Yj24—Yangjiang 24 subsag; Ep19—Enping 19 subsag; Ep 20—Enping 20 subsag; Ep 21—Enping 21 subsag; Ep27—Enping 27 subsag.

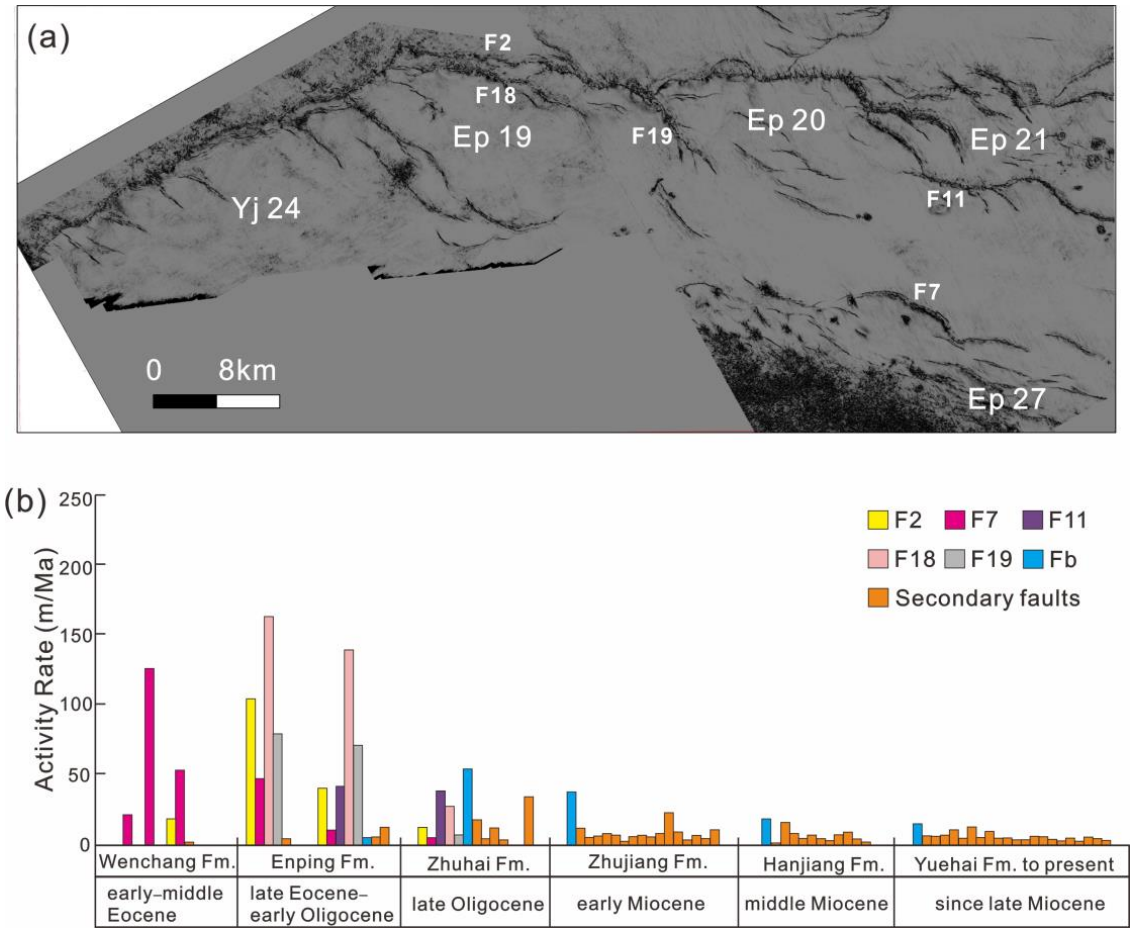

Figure 4. Fault patterns of East Yangjiang Sag shown in time slice at 1500ms (**a**) (see Figure 3 for locations), and the dip–slip active rate of major NW-trending faults in the Zhu III Depression (**b**). The data of the secondary faults are from [22].

During the late Eocene–early Oligocene rifting II period of the Yangjiang Sag, the number of NW-direction faults significantly increased. Among these, pre-existing major faults, such as the NW-trending F7, F19, and F20 faults, were characterized by inherited activity. However, their activity intensity changed during this stage, as represented by the reduced intensity of F7 activity. In addition, a few new major faults formed at this stage. The F18 was formed and was active as a branch fault of F1 at the highest rate of ~170 m/Ma. This led to a transition of the Enping 19 subsag from a single half-graben to a composite half-graben in the north–south double-fault model. Additionally, another southward dipping major fault F11 formed in a NNW trend, and its strong activity caused the rifting of the Enping 20 subsag to move southwards continuously. On the sides of the active major faults in both the NE and NW trends, some newly generated faults with NWW trending were developed and combined into en echelon structures and horsetail structures horizontally. The newly generated faults cut the Enping Formation with a thickness difference between the two sides of the faults, indicating the extensional characteristics. In addition, several secondary faults in a NW trend formed cross the sag diagonally. In a cross-section, the faults were identified as forming step-shaped, Y-shaped, and negative flower structural styles (Figure 5), manifesting strike–slip characteristics.

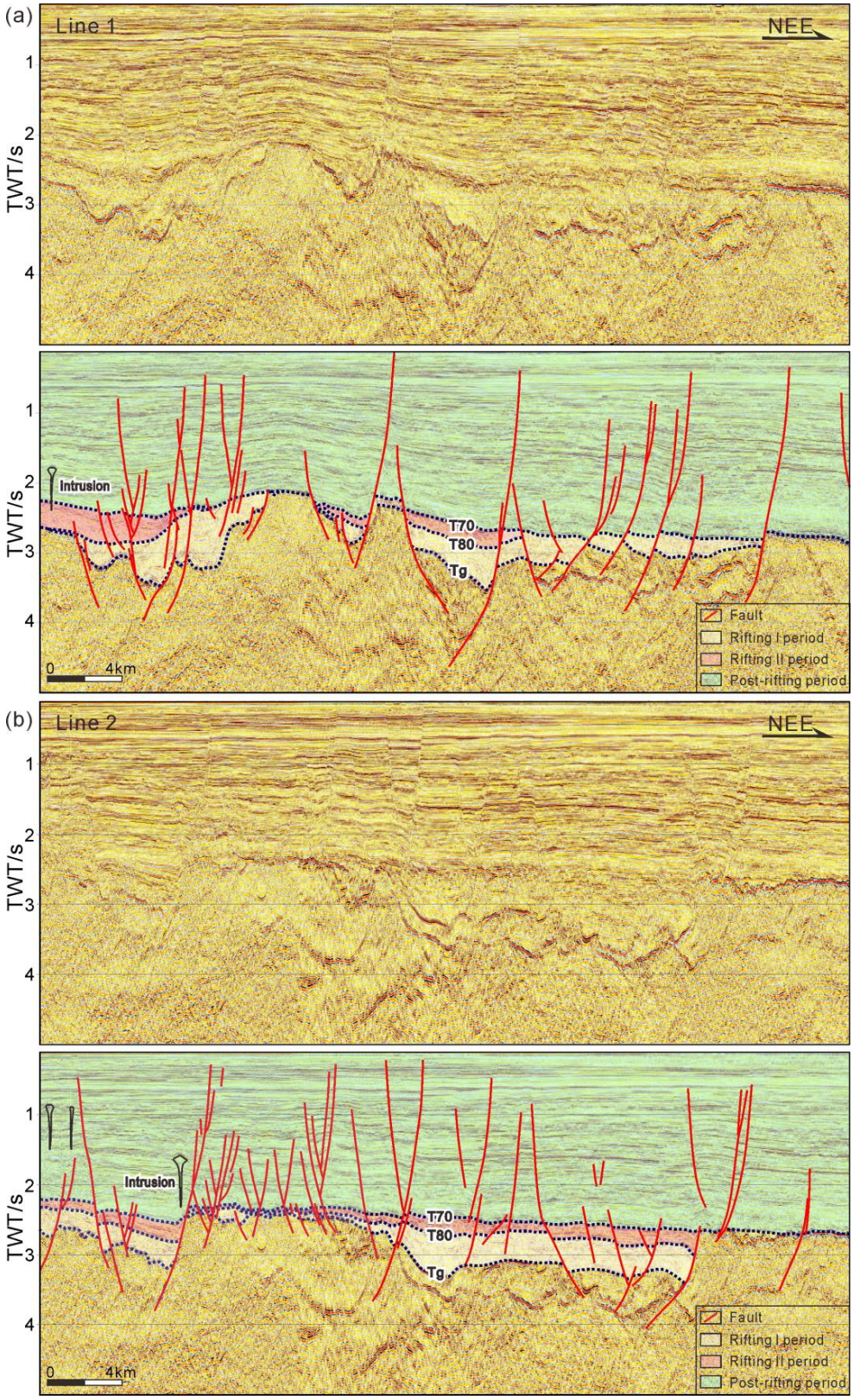

Figure 5. Fault system and structural style showed in the seismic profiles of the Yangjiang Sag, with corresponding unexplained seismic profiles (see Figure 3 for locations). The (**a**,**b**) corresponds the profile in Lines 1, 2. The rifting I period corresponds to the First Zhu–Qiong Movement in early–middle Eocene and the sedimentation of the Wenchang Formation in the basin, while the rifting II period corresponds to the Second Zhu–Qiong Movement in late Eocene when the Enping Formation developed.

In the post-rifting period since late Oligocene, there was a significant decrease in the number of NE- and nearly E–W-oriented faults, while the NW-oriented fault system emerged as the dominant feature within the sag (Figure 4a). The formation of this fault system can be attributed to the continuous expansion and linkage of the initially formed short NW-oriented faults from the rifting stage. Additionally, some new NW-oriented faults developed around pre-existing ones, merging to form Y-shaped patterns and negative flower structures, as shown in Figure 5. These newly formed faults, located in the shallow layer, exhibit minor fault displacement, with virtually no variation in the formation thickness between the two sides. This means that the extensional intensity of the fault activity was obviously weakened, while the strike–slip component dominated. During this stage, on the Yangchun Uplift in the north of the Yangjiang Sag, some steep and erect NW-trending faults developed, which often cut down to the basement. Negative flower structures were also identified in this section, and the fault throws of these faults are relatively small, showing the characteristics of strike–slip motion.

4.2. Fault Patterns of the Wenchang Sag

Under the influence of the Zhu III South Fault's activity, the Wenchang Sag commenced its rifting process during the Paleocene, marking it as the earliest sag formation within the Zhu III Depression. During the rifting I period of the sag, the dominant fault was the NE-oriented Zhu III South Fault (Fa). This fault, characterized by segmented activity, governed the development of secondary sags, namely, Wenchang A, B, and C sags. Simultaneously, the NW-oriented No. 3 fault (Fb), which emerged within the Wenchang B sag, served as an eastward-dipping extensional fault, thereby segmenting the sag's internal structure (Figure 6).

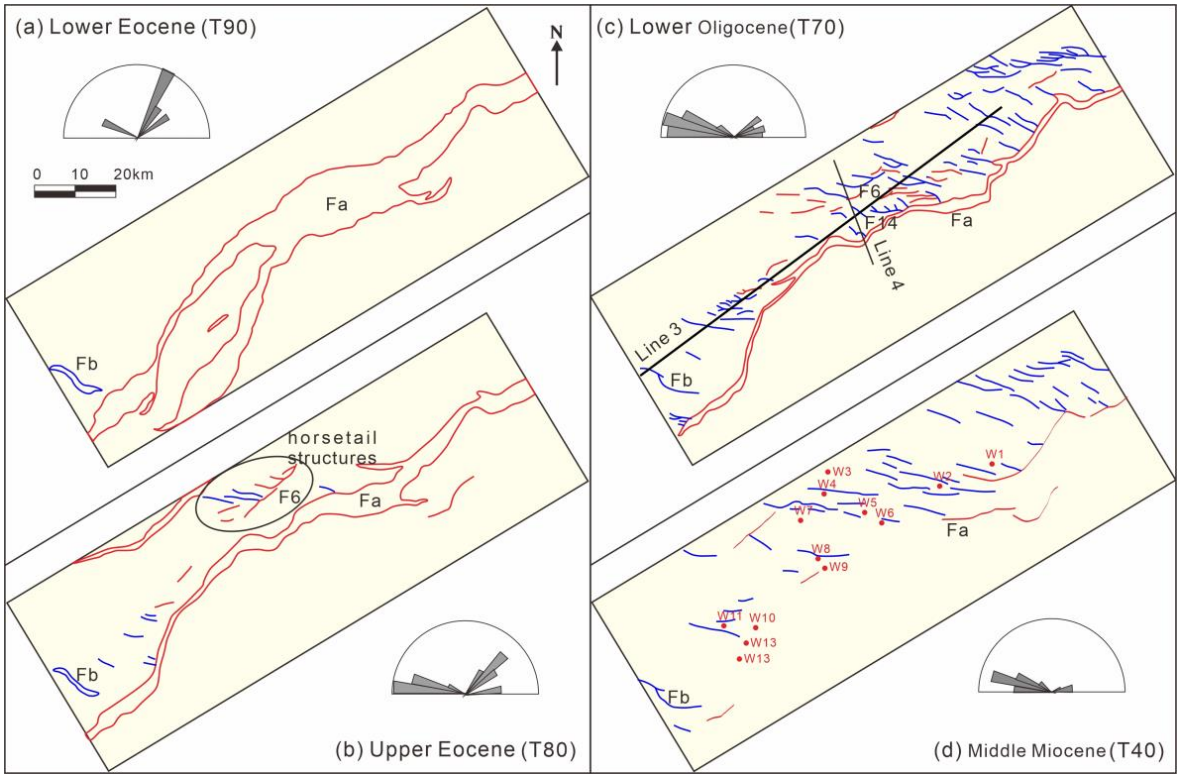

Figure 6. Fault patterns and rose diagram in different seismic reflectors of the Wenchang Sag. The rose diagram is drawn based on statistical analysis of the fault strikes. The fault data are from [37], and the well data are from [59]. The red lines represent the NE- to EW-trending faults, and the blue lines represent the NW-oriented faults. Fa represents the Zhu III south fault, and Fb represents the No. 3 fault in the Wenchang B Sag.

During the rifting II period of the Wenchang Sag, faults with nearly E–W and NWW orientations were not only generated but also increased in number. These faults are curved in shape and relatively short in length, most of which show left-stepping en echelon assemblage in plan view. Furthermore, some of the NWW-oriented faults laterally connect with the NE-oriented faults, forming horsetail structures. These structures are particularly well-developed near the F6 fault belt in the Wenchang A sag. In the seismic section, it is observed that the fault surfaces mostly tilt northward and are distributed in a stepped combination. Some faults can extend downwards and link to the NE-trending major fault or sag-controlling fault, forming Y-shaped patterns (Figure 7). It is implied that the dextral strike–slip motion might take place along the NE-trending fault by the geometric and kinematic analysis, which is similar to that in the Yangjiang Sag. Additionally, the NW-oriented faults, which cut through the Enping Formation, function as synsedimentary normal faults and contribute to the evolution of the depocenter.

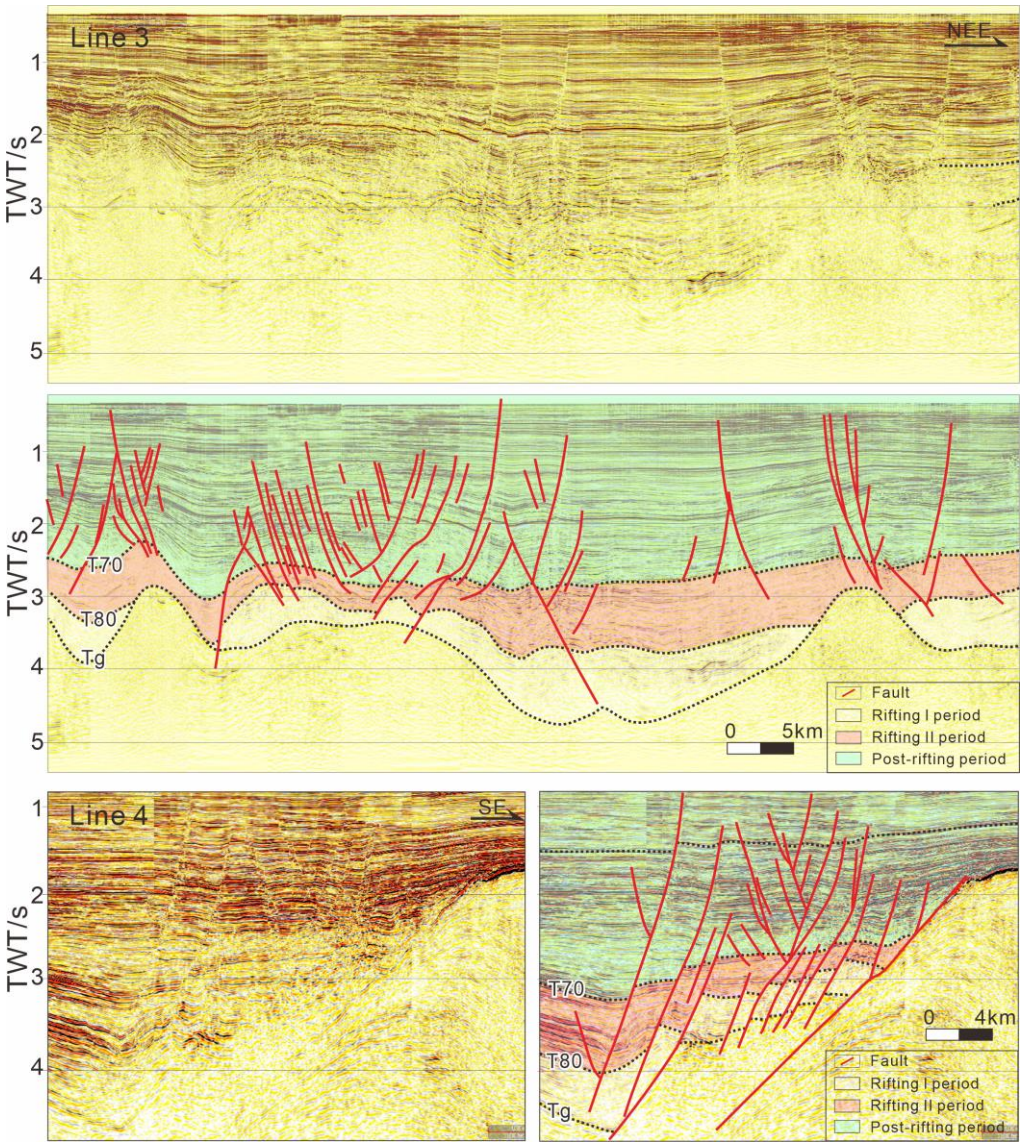

Figure 7. Fault system and structural style shown in the seismic profiles of the Wenchang Sag, with corresponding unexplained seismic profiles (see Figure 6 for locations; the seismic data are from [22,32]).

In the post-rifting period, the NW-oriented faults became dominant within the depression, coinciding with the cessation of activity in the early NE- and nearly E–W-oriented faults. Although the number of active faults in this stage significantly decreased, the scale and length of the faults expanded compared to that in the previous stage. The NW-trending faults mostly appear in straight rather than curved shapes in plan view. The newly formed NW-trending faults are mostly arranged in en echelon and combine with the early faults in Y-shaped and negative flower structures on the profile. It can also be seen that the NW-trending faults have smaller fault throws, meaning that the activity of the fault weakens, and the depression enters the stage of thermal subsidence as a whole.

5. Discussion

5.1. Development Stages of NW-Trending Faults

As shown in the rose diagram of the fault strikes (Figures 3 and 6), the orientations of the Cenozoic faults in the Zhu III Depression underwent a transition from NE (T80) to nearly E–W (T70), and subsequently to NWW (T40). This change reflects a clockwise rotation of the regional extension direction from NW–SE to N–S to NNE–SSW. Under the dextral transtensional stress setting, the direction of primary rotational main extensional stress intersects obliquely with the strike of pre-existing basement faults or pre-formed main controlling faults. This intersection can induce oblique extension or strike–slip activity of early faults in the basin [55]. Consequently, the NW-oriented faults, which started forming during the basin's initial rifting stage and continued to develop and dominate in the post-rifting stage, could exhibit varying activity characteristics under the regional dextral transtensional stress conditions.

Given the geometric and kinematic characteristics of faults, it becomes apparent that NW-oriented faults exhibit significant variations across different structural layers. The NW-oriented faults, which developed in the deep layers (Shenhu and Wenchang formations) were major sag-controlling faults during the rifting I period. They are small in number and exhibit strong continuity, large fault displacement, and a shovel-shaped fault surface, indicative of synsedimentary boundary faults. At this stage, however, the dominant faults are mainly developed in the NE orientation, especially reflected in the boundary faults. The number of faults in the Enping Formation has increased, and the faults are distributed in belts in plan view, arranged in en echelon, and connected laterally to the early NE-trending major faults. Vertically, the newly generated faults form a Y-shaped combination with the major faults, and the negative flower structures also developed, all of which reveal that the NW-trending faults were characterized by strike–slip motion in the rifting II period. A fault displacements analysis reveals that the activity intensity of the newly formed major faults was greater than that in the rifting I period. Furthermore, secondary faults played a significant role in controlling the sedimentation of the Enping Formation. It can be seen that main motion of the faults developed in this stage is extension with dextral slip component.

Within the shallow structural layers of the post-rifting stage, the newly formed faults primarily exhibit a NW orientation and are predominantly arranged in an en echelon pattern. The fault surfaces present as nearly vertical, high-angle structures with minimal fault displacement, as observed on the profile. Additionally, negative flower structures were developed. It is reasonable to infer that the NW-trending faults in this stage are mainly characterized by strike–slip motion. Taking the changing dynamics of the regional stress field into account, the evolution of the NW-oriented faults in the Zhu III Depression can be segmented into three stages: the extension stage during rifting I period, the extension–strike–slip stage during rifting II period, and the strike–slip stage during the post-rifting period. The newly formed faults in different stages correspond to different genetic types and mechanisms.

5.2. Genetic Types and Formation Mechanism

According to the structural analysis on seismic profiles, two groups of pre-Cenozoic faults were identified in the basement, which manifested as conjugate pre-existing fault

systems trending in the WNW and ENE directions (Figure 8). The conjugate fault systems appear as imbricate and flat-ramp fault structures on the section, suggesting the development of thrust fault systems during the pre-Cenozoic. The ENE-trending thrust faults cuts the WNW-trending thrust faults on the seismic reflection profile, indicating it formed at a relatively later stage and preserved more completely. The thrust faults trending in ENE and WNW have been also suggested to be widespread in the basement of the Zhu I and Zhu II depressions, based on the borehole-constrained high-quality 3D seismic data [18,19,27,60,61]. Additionally, it was also discovered that the boundary faults and some major normal faults within the Cenozoic basin cut through the Tg and converged with the pre-existing faults, similar to that in the Enping and Baiyun sags. It is concluded that the pre-rifting structure played a key role in controlling the architecture and rifting of the PRMB.

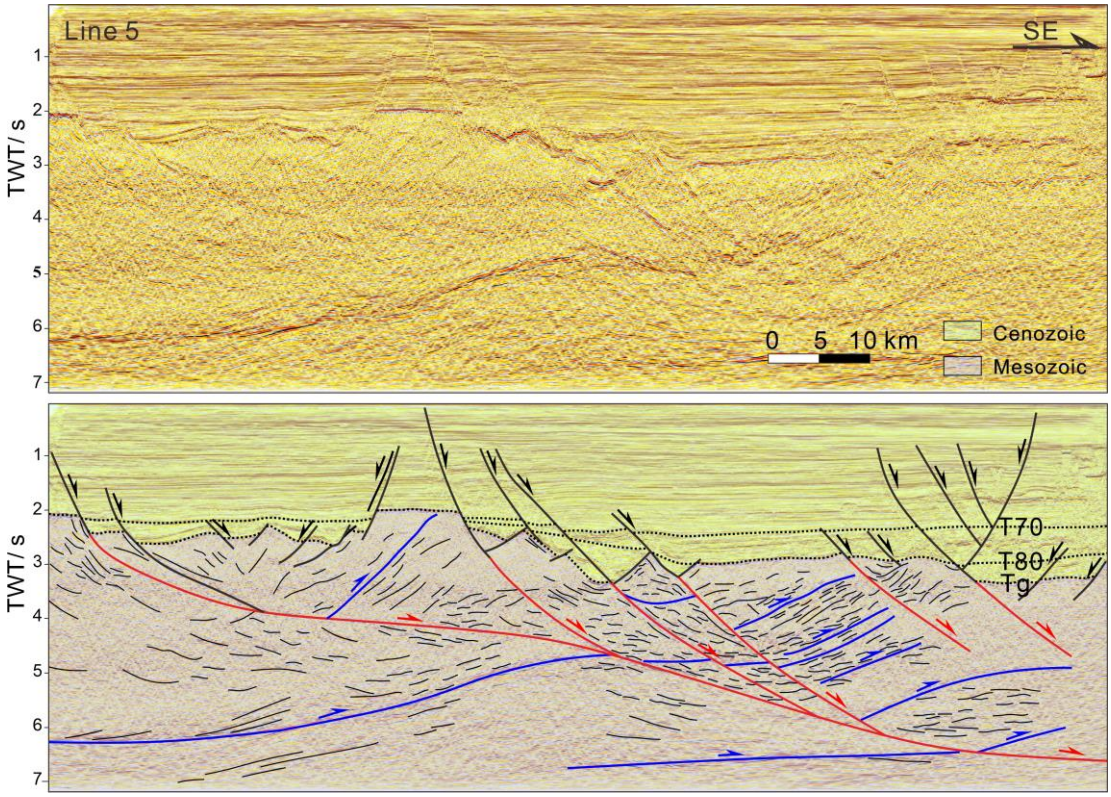

Figure 8. The distribution of pre-existing structures in the basement of the Yangjiang Sag and their relationship with the development of Cenozoic faults in the basin (see Figure 3 for location). The red lines represent the ENE-trending normal faults in the basement, which were reactivated and inverted from Mesozoic thrust faults during the Cenozoic. The blue lines represent the WNW-trending Mesozoic thrust faults, while the black lines represent the Cenozoic faults in the basin.

As previously mentioned, during the initial rifting of the Zhu III Depression, the primary extensional stress direction in the region was NW–SE. This led to the formation of a fault system primarily composed of NE-oriented faults (Figures 3 and 6). Concurrently, there are also a few conjugate NW–NWW-trending faults formed within sags as sag-controlling boundary faults. These faults manifest as curved structures in plan view and exhibit substantial fault displacement in cross-section, reflecting the characteristics of extensional faults. Moreover, they extend downwards and connect to the pre-existing basement faults. It is plausible to infer that the formation of NW-oriented faults during the rifting I period was closely associated with the reactivation of pre-existing NW-oriented faults in the basement. That is to say, under the background of NW–SE regional extension, the NE oriented pre-existing faults in the basement will be preferentially activated, forming

boundary faults in a NE trend that controlled the development of the initial depression. Meanwhile, the conjugate NW-trending faults, as weak structural zones in the basement, will also partially activate to form several NW–NWW-trending boundary faults and some secondary faults within the depression (Figure 9a,b). Consequently, the formation of NW-oriented extension faults during the Zhu III Depression's rifting I period can likely be attributed to the reactivation of the basement faults.

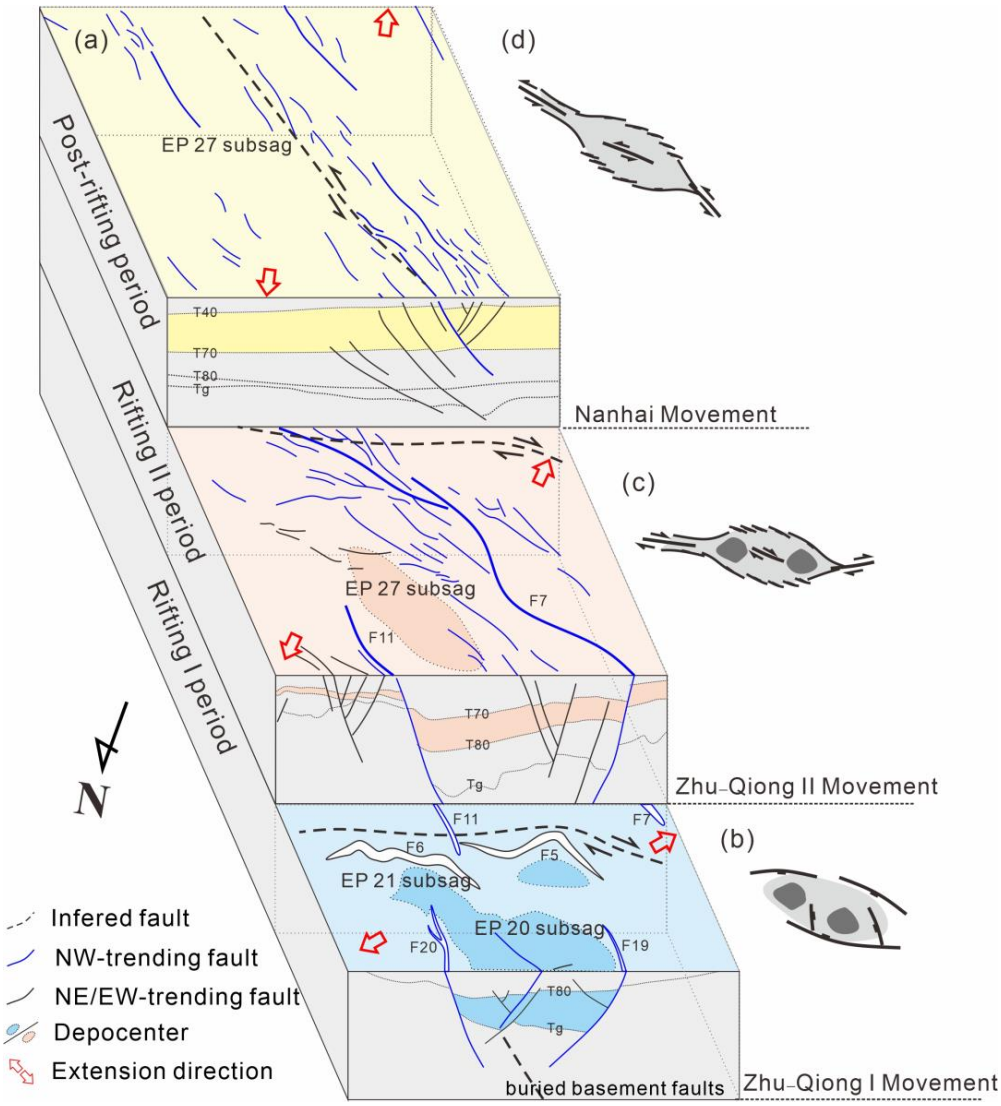

Figure 9. Simplified model showing three-stage evolution process of the NW-trending faults. Sub-figures (**a**) displays the three evolutionary stages in the form of spatial superposition to reveal the vertical correlation of the faults and the southward migration of sedimentary center. The ideal model on the right side of the map show the tectonic evolution mechanism of the extensional basin (**b**), transtensional basin (**c**), and strike–slip basin (**d**), and the connections between faults also can be explained.

During the rifting II period, the regional extension direction experienced a dextral shift, transitioning to nearly an S–N orientation. Meanwhile, the NE-trending strike–slip fault systems have been revealed to develop in the marginal basin on the NSCS, according to a structural analysis of field and seismic data and numerical modeling [35,56,62,63]. Accompanied by the faults in the nearly E–W direction dominant at this period, the number of NWW-oriented faults increased. These NWW-oriented faults displayed left-stepping en echelon arrangements and were predominantly connected to boundary faults, forming

horsetail structures. This suggests that the newly formed faults likely resulted from dextral strike–slip motion along the major NE-oriented faults. Moreover, the faults also showed a stepped combination on the profile and formed Y-shaped and negative flower-shaped structures with the boundary fault, all of which could prove the development of strike–slip structures in the depression. In particular, within the East Yangjiang Sag, the NE-oriented boundary faults give rise to dextral pull-apart structures [24]. Consequently, a secondary NW-oriented strike–slip fault zone is established along the diagonal of the rhombic-shaped Enping 20 subsag. Similarly, in the Wenchang Sag, the combination styles of the nearly E–W- and NWW-trending faults also revealed that the NE-trending major faults, represented by the Zhu III South Fault, experienced dextral strike–slip motion. The newly formed NWW-oriented synsedimentary faults penetrate downwards through the T80 reflector, suggesting that strike–slip activity commenced during the rifting II period (Enping Formation period). This contrasts with previous assertions that dextral transtensional faults emerged in the late Oligocene to early Miocene [26,55]. Due to the clockwise rotation of the regional extensional stress direction, the strike of boundary faults formed in the early stage, mainly oriented in the NE direction (basement structural line direction), has an oblique intersection with the direction of regional extensional stress. As the included angle of the oblique intersection continuously decreases, it prompts a gradual amplification of the dextral shear component produced by the active NE-oriented faults, thereby inducing dextral strike–slip activity. As a result, faults in E–W and NWW directions were derived within the depression, forming broom structures with the major faults, or left-stepping en echelon assemblages by lateral connection, which is consistent with the model of dextral transtensional basin (Figure 9c). Hence, the NWW-oriented faults that developed during this stage can likely be classified as strike–slip-derived types along the NE-oriented faults, characterized by extension with dextral strike–slip action (Figure 9a).

During the post-rifting stage, the basin entered the stage of thermal subsidence. There is weak fault activity from late Oligocene to early Miocene, which was known as a transition period [43,45]. The regional extensional direction shifted to NNE–SSW, leading to the formation of a fault system primarily composed of NW-oriented faults. The activity intensity of the NE- and nearly E–W-oriented faults formed during the rifting period significantly decreased or even ceased, while some NWW-oriented faults demonstrated continued activity. However, the activity intensity also weakened with the basin entering the depression period. During the Neotectonic period, there was an obvious rise in activity intensity of the NW-trending faults, which resulted in complex fault block activity in the region (Figure 4b). The Y-shaped and negative flower structures formed by the newly developed NWW-oriented faults and earlier faults in the profile, along with the right-stepping en echelon arrangement, suggest the evolution of the NW-oriented sinistral strike–slip faults. The NW-trending strike–slip activity was also highly developed in the uplift areas, such as the Qionghai Uplift, manifested as a single fault with a high angle and upright plane, cutting through the Hanjiang Formation upwards, even shallower strata, down to the basement, generally [11,59]. Furthermore, the Yangjiang–Yitong fault zone has been recognized as an active sinistral strike–slip fault zone since the Early Oligocene [17,64–66]. This supports the assertion that the NW-oriented faults that developed during this stage were associated with strike–slip motion, trending NW under the NNE–SSW extensional setting. The faulting in this stage is most notably characterized by sinistral strike–slip, which is consistent with model of the strike–slip basin (Figure 9d). However, within the Zhu III Depression, there may not be a continuous main strike–slip zone. Instead, the strike–slip faults could be the product of strike–slip motion along the adjacent Yangjiang–Yitong fault zone.

5.3. Geodynamic Process

The PRMB is situated at the northern continental margin of the SCS, where the convergence of the Pacific Plate (Philippines Sea Plate), the Indo–Australian Plate, and the Eurasian Plate is located (Figure 1). Generally, the sequence of stress superposition across

different temporal domains within the same spatial domain, or the ratio of the intensities of various superimposed stresses within the same temporal domain, can lead to substantial variations in the ultimate structural characteristics [67]. Hence, study of the PRMB's tectonic evolution dynamics should consider the two major geodynamic processes: the Pacific–Eurasian subduction and the India–Eurasian collision. This is essential for gaining a deep understanding of the primary dynamic sources driving the various stages of basin evolution.

In the early Eocene, the Indian Plate underwent rapid subduction and collision with the Eurasian Plate [68–70]. Concurrently, the subduction rate of the Pacific Plate, trending NNW, decreased, initiating the retreat of the subduction zone [71]. This led to a transition of the tectonic regime in the NSCS from compression to NW–SW extension. Under the extensional background, the Zhu III Depression in the PRMB began to rift, and major NE-oriented faults developed due to the preferential reactivation of pre-existing NE-oriented faults in the basement. Meanwhile, a few NW-trending pre-existing faults in the basement also reversed and reactivated [18,56] to form the first period of NW-trending extensional faults by tectonic inversion. Since the late Eocene, the subduction direction of the Pacific Plate shifted from NNW to NWW toward the southeastern edge of the Eurasian Plate [71–73]. The ongoing India–Eurasia collision and the oblique subduction between the Pacific and Eurasian plates have led to the formation of a dextral transtensional tectonic setting in the NSCS [74,75]. Dextral strike–slip motion occurred along the NE-oriented major faults within the basin. This triggered the development of NW-oriented secondary faults, characterized by both extension and strike–slip movements. In the Early Oligocene, the continuous collision of the India–Eurasian plate caused lateral extrusion of the Indochina Block southeastwards. Meanwhile, slab pull due to southward subduction of the proto-SCS caused breakup of the NSCS and spreading of the SCS [8,68]. A widespread transition from rifting to post-rifting thermal subsidence occurred in the NSCS where the post-rift fault activities are widely distributed [64,76]. The Zhu III Depression in the PRMB entered the depression period, accompanied by the weakening fault activity. The activity of NW-trending faults became the dominant faults, exhibiting sinistral strike–slip motion. In middle Miocene, the arc–continent collision ended the spreading of the SCS, and the sustained subduction of Philippine Sea Plate towards the Eurasian Plate resulted in compressive uplift and erosion in the PRMB.

5.4. Significance on Basin Evolution

The inversion-related extensional faults trending NW formed during the rifting I period have a relatively limited distribution within the Zhu III Depression. They primarily play the role of boundary faults that control the development of sags or subsags. The F19 and F20 faults, acting as synsedimentary faults, bound the Enping 20 subsag of the Yangjiang Sag. These faults cut through the Tg interface with significant fault throws, playing a crucial role in the deposition processes of the Wenchang Formation and restricting the spatial distribution and morphological development of the sag. The development of the F18 fault, the boundary fault in the north of the Enping 19 subsag, has transformed the subsag from an initial half-graben with northern-faulted and southern-overlapped patterns to a double-faulted graben. In addition, the F7 fault located in the southern Yangjiang Sag is the main controlling fault of the Enping 27 subsag. The fault was formed in the upper Wenchang Formation period, causing the depocenter of the Yangjiang Sag to migrate southwards. Similarly, the No. 3 fault located in the Wenchang B sag is a segmented fault of the Wenchang depression zone, controlling the development of the internal tectonic and sedimentation. It is evident, therefore, that the NW-oriented faults formed during the rifting I period exert a significant influence on the division of internal structural units, the evolution of local tectonics, and the development of the depression's depocenter.

The NW-oriented faults, resulting from dextral strike–slip movements, developed during the rifting II period. Despite their wide distribution within the depression, the size of individual faults is generally relatively small. As a product of the strike–slip activity of

NE–NEE-trending boundary faults/major faults, they regulated the continuous dextral extensional stress at the beginning of strike–slip motion, and derived extension–strike–slip faults in the overlapping area of the main strike–slip faults. This increased the complexity of the local tectonic within the depression. Meanwhile, the NW-trending sag-controlling faults formed in the rifting I period continued to be active, causing the southward migration of the depocenter. Moreover, during this stage, the long-axis direction of deposition shifted from ENE to WNW, which is a response to the dextral transition of the regional stress field [21,27]. With the migration of the rifting and deposition, tectonic uplift took place in local areas. For example, with the steady strengthening of F11 fault activity, the Enping 21 subsag located in the footwall continuously tilted and uplifted, leading to the formation of a faulted nose structure and the erosion in the northern ramp of the Yangjiang Sag. In addition, the NW-oriented faults that formed during this stage intersected with earlier faults, leading to the creation of block traps. These became a significant type of oil and gas trap during the rifting period.

The NW-oriented strike–slip faults formed during the post-rifting stage predominantly developed within the Neogene sedimentary layer. These faults, defined by their short developmental periods and modest sizes, typically extend in length from hundreds to thousands of meters. Some of the faults could cut down to the basement with a high angle, complicating local structures in the depression. There are also differences in the activity intensity of NW-trending faults during this stage. During the early post-rifting stage, a period marked by tectonic tranquility, fault activity was generally subdued. In the late post-rifting, the activity of the fault enhanced (Figure 4) while the basin entered the tectonic activation period, which affected the activity of fault blocks in the depression and the formation of local structures. Additionally, fault activity during this stage significantly influenced the trapping, migration, and preservation of oil and gas. In the overlap region of the sinistral left-stepping faults in the Yangjiang Sag, a series of faulted nose and fault block traps were formed. Based on the drilling results, it has also been confirmed that the NW-trending fault is of good lateral seal ability and became a kind of trap-controlling fault in the oil fields of the Enping 20 subsag [23,24]. Furthermore, the NW-oriented faults can also facilitate the vertical migration of oil and gas to the Neogene Zhujiang Formation, thereby becoming a major conduit for oil and gas transportation within the Yangjiang Sag. Within the Wenchang Sag, the strengthening NW-oriented faults, in conjunction with the NE-oriented major faults, led to the formation of S-shaped, dextral left-stepping, and skew-shaped stress-increased traps [26]. These traps play a controlling role in the trapping and accumulation of hydrocarbons.

As mentioned above, the faults formed during the initial rifting stage of the basin are often basin-controlling or sag-controlling faults. The development of these faults determines the location, shape, and basic structural units of the early depression. The faults formed during the rifting II period played a controlling role in the migration of the basin's rifting and sedimentary centers, making the internal structure of the basin more complex. The faults in the post-rifting stage exhibit a general decrease in activity, with their influence on the basin structure being less pronounced. They induce fault block activity within certain uplifted areas. Moreover, the faults have a significant impact on oil and gas reservoirs. Early rifting faults control the distribution of source rocks and play a crucial role in providing channels for oil and gas transportation, especially the long-active faults, which facilitate the migration of oil and gas from deep to shallow layers. Some secondary faults are crucial for the lateral sealing of oil and gas, developing important structural traps. In addition, the fault activities in the post-rifting stage also have a significant impact on the trapping and migration of oil and gas reservoirs. However, it is worth noting that the impact has both advantages and disadvantages. While forming effective traps, it may also destroy existing oil and gas reservoirs.

In summary, the seismic data used in this study, underpinned by well-log correlations, constitute high-precision 3D seismic data. These data are instrumental in elucidating the sedimentary–structural characteristics of the Zhu III Depression. However, it is important

to note that the data distribution is confined to the Yangjiang and Wenchang Sags and does not extend to include other areas such as the Yangchun and Qionghai Sags. Moreover, our structural analysis is primarily grounded in the results derived from seismic section interpretation, though different time slices also prove extremely useful in unveiling strike–slip structures. Concurrently, a broader array of methods, including physical simulation, can be employed to examine the formation and evolution of strike–slip structures. These methodologies will continue to be integrated into our ongoing research efforts.

6. Conclusions

Based on a detailed structural analysis of the Zhu III Depression of the Pearl River Mouth Basin, we arrive at the following conclusions.

Considering their geometric and kinematic characteristics, as well as the regional dextral extensional stress setting, the NW-oriented faults can be classified into three evolutionary stages: extension in Palecene to middle Eocene, dextral transtension during late Eocene to early Oligocene, and sinistral strike–slip since late Oligocene.

The NW-trending extensional fault represents a type of tectonic inversion, triggered by the reactivation of basement faults. The transtensional faults are strike–slip-derived faults, resulting from dextral strike–slip motion of the NE-trending major faults under the regional dextral extensional stress setting. The strike–slip fault is caused by the sinistral shearing action related to the lateral extrusion of the Indochina Block and slab pull of the proto-SCS subduction.

The NW-oriented extensional faults in the rifting I period influenced the division of sag structures and depocenter distribution. The late Eocene–early Oligocene transtensional faults controlled the local tectonic development within the depression and the formation of oil and gas structural traps, as well as depocenter migration. The sinistral strike–slip faults affected the activity of fault blocks, along with the trapping, migration, and preservation of oil and gas since late Oligocene.

In our future work, more time slices will be applied to explore strike–slip faults. Concurrently, we aim to establish relationships between major and minor faults through simulation experiments. We will also focus on the study of strike–slip faults' influence on the migration and storage of oil and gas and formulate a strike–slip controlled reservoir model.

Author Contributions: Conceptualization, L.Z. and D.M.; Methodology, P.Z., L.Z., J.Z., D.M. and Y.C.; Software, P.Z. and L.Z.; Validation, L.Z. and Y.C.; Formal analysis, P.Z., L.Z., J.Z., D.M., Y.C. and P.R.; Investigation, J.Z. and D.M.; Resources, L.Z. and J.Z.; Data curation, P.Z., J.Z., D.M., Y.C. and P.R.; Writing—original draft, P.Z. and L.Z.; Writing—review & editing, P.Z., L.Z., J.Z., D.M., Y.C. and P.R.; Visualization, P.Z., Y.C. and P.R.; Supervision, D.M. and P.R.; Funding acquisition, L.Z. and D.M. All authors have read and agreed to the published version of the manuscript.

Funding: This work was financially supported by Natural Science Foundation of Shandong Province of China (No. ZR2022QD079), the Project of Introducing and Cultivating Young Talent in the Universities of Shandong Province (No. LUJIAOKEHAN–2021–51, granted to L. Yu), and the Scientific Research Start Funds Project of the Fourth Institute of Oceanography, Ministry of Natural Resources (No. 202106).

Institutional Review Board Statement: Not applicable.

Informed Consent Statement: Not applicable.

Data Availability Statement: Data are contained within the article.

Conflicts of Interest: The authors declare no conflict of interest.

References

1. Wu, Z.P.; Li, W.; Ren, C.J.; Li, C.S. Basin Evolution in the Mesozoic and Superposition of Cenozoic Basin in the area of the Jiyang Depression. *Acta Geol. Sin.* **2003**, *77*, 280–286. (In Chinese with English Abstract)
2. Quan, Y.B.; Liu, J.Z.; Zhao, D.J.; Hao, F.; Wang, Z.F.; Tian, J.Q. The origin and distribution of crude oil in Zhu III sub-basin, Pearl River Mouth Basin, China. *Mar. Pet. Geol.* **2015**, *66*, 732–747. [CrossRef]

3. Liu, L.; Sun, Y.H.; Chen, C.; Lou, R.; Wang, Q. Fault reactivation in No.4 structural zone and its control on oil and gas accumulation in Nanpu sag, Bohai Bay Basin, China. *Pet. Explor. Dev.* **2022**, *49*, 824–836. [CrossRef]
4. Allgaier, F.; Busch, B.; Hilgers, C. Fault leakage and reservoir charging in the Upper Rhine Graben, Germany—Assessment of the Leopoldshafen fault bend. *Mar. Pet. Geol.* **2023**, *156*, 106428. [CrossRef]
5. Sobhy, H.; Moustafa, A.R. Impact of structural geometry of tilted fault blocks on hydrocarbon entrapment and deposition of syn–rift clastic reservoirs: Belayim Marine field (Gulf of Suez rift). *Mar. Pet. Geol.* **2024**, *160*, 106631. [CrossRef]
6. Bashmagh, N.M.; Lin, W.R.; Radwan, A.E.; Manshad, A.K. Comprehensive analysis of stress magnitude and orientations and natural fractures in complex structural regimes oil reservoir: Implications for tectonic and oil field development in the Zagros suture zone. *Mar. Pet. Geol.* **2024**, *160*, 106615. [CrossRef]
7. Sun, Z.; Zhong, Z.H.; Keep, M.; Zhou, D.; Cai, D.S.; Li, X.S.; Wu, S.M. 3D analogue modeling of the South China Sea: A discussion on breakup pattern. *J. Asian Earth Sci.* **2009**, *34*, 544–556. [CrossRef]
8. Wang, P.C.; Suo, Y.H.; Peng, G.R.; Li, S.Z.; Du, X.D.; Chao, X.Z.; Zhou, J.; Wang, G.Z.; Santosh, M.; Jiang, S.H.; et al. Three-stage extension in the Cenozoic Pearl River Mouth Basin triggering onset of the South China Sea spreading. *Gondwana Res.* **2023**, *120*, 31–46. [CrossRef]
9. Nguyen, H.H.; Carter, A.; Hoang, L.V.; Fox, M.; Pham, S.N.; Vinh, H.B. Evolution of the continental margin of South to Central Vietnam and its relationship to opening of the South China Sea (East Vietnam Sea). *Tectonics* **2022**, *41*, e2021TC006971. [CrossRef]
10. Lei, B.H.; Zheng, Q.G.; Li, J.L.; Liu, H.; Wang, H.R. Formation and evolution of Zhu-3 south fault and its control on the depocenter shift in Zhu-3 depression, Pearl River Mouth Basin. *Acta Geol. Sin.* **2012**, *33*, 807–813. (In Chinese with English Abstract)
11. Li, H.; Zhang, Y.Z.; Gan, J.; Lu, J.; Zhan, Z.P. The style distribution and hydrocarbon accumulation of inverted structures in Zhu-3 depression. *J. Oil Gas Technol.* **2014**, *36*, 1–6.
12. Quan, Y.B.; Liu, J.Z.; Hao, F.; Bao, X.H.; Xu, S.; Teng, C.Y.; Wang, Z.F. Geochemical characteristics and origins of natural gas in the Zhu III sub-basin, Pearl River Mouth Basin, China. *Mar. Pet. Geol.* **2018**, *101*, 117–131. [CrossRef]
13. Heinemann, N.; Haszeldine, R.S.; Shu, Y.T.; Stewart, R.J.; Scott, V.; Wilkinson, M. CO_2 sequestration with limited sealing capability: A new injection and storage strategy in the Pearl River Mouth Basin (China). *Int. J. Greenh. Gas Control* **2018**, *68*, 230–235. [CrossRef]
14. Fu, X.Y.; Chen, S.J.; You, J.J.; Li, H.; Lei, M.Z. Geochemical characteristics and sources of crude oil in the Wenchang B depression and the Western Qionghai uplift of the Zhu-3 sub-basin, Pearl River Mouth Basin, South China Sea. *J. Pet. Sci. Eng.* **2022**, *219*, 111091. [CrossRef]
15. Zheng, Q.G.; Li, J.L.; Lei, B.H.; Song, P.; Li, Q.; Shi, D.F.; Liu, H.; Lin, C.S. Differential tectonic evolution and formation mechanism of three subsags in Wenchang Sag of Pearl River Mouth Basin, South China Sea. *Pet. Sci.* **2023**, *20*, 1379–1394. [CrossRef]
16. Ge, J.W.; Dong, Y.L.; Tan, M.X.; Chen, H.H.; Sun, L.P.; Shun, L.P.; Li, S.L.; Zhao, X.M. Tecono-stratigraphy of Paleogene Zhu-3 depression of the Pearl River Mouth Basin, South China Sea: Implications for syn-rift architecture in multiphase rifts. *Mar. Pet. Geol.* **2023**, *155*, 106389. [CrossRef]
17. Wang, J.H.; Pang, X.; Tang, D.Q.; Liu, B.J.; Xu, D.H. Transtensional tectonism and its effects on the distribution of sandbodies in the Paleogene Baiyun Sag, Pearl River Mouth Basin, China. *Mar. Geophys. Res.* **2013**, *34*, 195–207. [CrossRef]
18. Ye, Q.; Mei, L.F.; Shi, H.S.; Camanni, G.; Shu, Y.; Wu, J.; Yu, L.; Deng, P.; Li, G. The Late Cretaceous tectonic evolution of the South China Sea area, An overview, and new perspectives from 3D seismic reflection data. *Earth Sci. Rev.* **2018**, *187*, 186–204. [CrossRef]
19. Suo, Y.H.; Li, S.Z.; Peng, G.R.; Du, X.D.; Zhou, J.; Wang, P.C.; Wang, G.Z.; Somerville, I.; Diao, Y.X.; Liu, Z.Q.; et al. Cenozoic basement-involved rifting of the northern South China Sea margin. *Gondwana Res.* **2022**, *120*, 20–30. [CrossRef]
20. Li, G.; Mei, L.F.; Pang, X.; Zheng, J.Y.; Ye, Q.; Hao, S.H. Magmatism within the northern margin of the South China Sea during the post-rift stage: An overview, and new insights into the geodynamics. *Earth-Sci. Rev.* **2022**, *225*, 103917. [CrossRef]
21. Mu, D.L.; Peng, G.R.; Zhu, D.W.; Li, S.Z.; Suo, Y.H.; Zhan, H.W.; Zhao, L.T. Structure and formation mechanism of the Pearl River Mouth basin: Insights from multi-phase strike-slip motions in the Yangjiang Sag, SE China. *J. Asian Earth Sci.* **2022**, *226*, 105081. [CrossRef]
22. Wu, W.Q.; Li, W.; Fan, C.W.; Li, H.; Li, M.; Li, J.; Zhao, Y.L.; Meng, M.F. Control of the Cenozoic transformation in regional extension direction on the development and evolution of fault system in Zhusan Depression. *Mar. Geol. Front.* **2023**, *39*, 52–65. (In Chinese with English Abstract)
23. Du, X.D.; Peng, G.R.; Wu, J.; Zhang, Z.W.; Xu, X.M.; Zhu, D.W. Faults and Its Impacts on Petroleum Accumulation in Eastern Yangjiang Sag, Pearl River Mouth Basin. *Xinjiang Pet. Geol.* **2020**, *41*, 414–421. (In Chinese with English Abstract)
24. Liu, J.; Peng, G.R.; Zhu, D.W.; Wu, J.; Zhang, Z.W.; Du, X.D.; Wang, X.M.; Liu, Q.Y.; Li, S.Z.; Suo, Y.H. Fault-controlled Hydrocarbon Accumulation in the Eastern Yangjiang Sag, Pearl River Mouth Basin. *Geotecton. Metallog.* **2021**, *45*, 123–130. (In Chinese with English Abstract)
25. Zhang, Y.C.; Gan, J.; Li, H.; Yuan, B.; Deng, G.J.; Zheng, R.F.; Wu, Y.Y.; Cao, Z. Strike-slip deformation mechanism and its petroleum geology significance along south fault in Zhu III depression under extensional tectonic setting. *China Offshore Oil Gas* **2013**, *25*, 9–15. (In Chinese with English Abstract)
26. Jiang, R.F.; Zhou, J.X.; Yang, X.B.; You, J.J.; Li, S.S.; Chen, L.; Zhang, X. The different extension and strike-slip mechanism and its accumulation controlling effect in Wenchang B sag. *Acta Geol. Sin.* **2020**, *94*, 2422–2432. (In Chinese with English Abstract)

27. Zhan, H.W.; Wang, G.Z.; Peng, G.R.; Suo, Y.H.; Wang, P.C.; Du, X.D.; Zhou, J.; Li, S.Z.; Zhu, D.W. Cenozoic evolution of the Yangjiang-Yitong'ansha fault zone in the northern South China Sea: Evidence from 3D seismic data. *Front. Earth Sci.* **2023**, *10*, 1070004. [CrossRef]
28. Clift, P.; Lin, J. Preferential mantle lithospheric extension under the South China margin. *Mar. Pet. Geol.* **2001**, *18*, 929–945. [CrossRef]
29. Xie, X.N.; Ren, J.Y.; Wang, Z.F.; Li, X.S.; Lei, C. Difference of tectonic evolution of continental marginal basins of South China Sea and relationship with SCS spreading. *Earth Sci. Front.* **2015**, *22*, 77–87.
30. Barckhausen, U.; Engels, M.; Franke, D.; Ladage, S.; Pubellier, M. Reply to chang et al. 2014, evolution of the South China Sea: Revised ages for breakup and seafloor spreading. *Mar. Pet. Geol.* **2015**, *59*, 679–681. [CrossRef]
31. Wen, Y.L.; Li, C.F.; Wang, L.J.; Liu, Y.T.; Peng, X.; Yao, Z.W.; Yao, Y.J. The onset of seafloor spreading at the northeastern continent-ocean boundary of the South China Sea. *Mar. Pet. Geol.* **2021**, *133*, 105255. [CrossRef]
32. Wang, Z.Z.; Hu, L.; Wang, S.C.; Lei, M.Z.; Li, M.; Hu, Q.M.; Liu, K. Structural characteristics and reservoir-control mechanism of Wenchang 9-7 transfer slope zone in Zhu III Depression, Pearl River Mouth Basin. *Mar. Orig. Pet. Geol.* **2023**, *28*, 83–93. (In Chinese with English Abstract)
33. Molnar, P.; Tapponnier, P. Relation of the tectonics of eastern China to the India-Eurasia collision: Application of slip-line field theory to large-scale continental tectonics. *Geology* **1977**, *5*, 212–216. [CrossRef]
34. Yin, A. Cenozoic tectonic evolution of Asia: A preliminary synthesis. *Tectonophysics* **2010**, *488*, 293–325. [CrossRef]
35. Xu, J.Y.; Ben-Avraham, Z.; Kelty, T.; Yu, H.S. Origin of marginal basins of the NW Pacific and their plate tectonic reconstructions. *Earth Sci. Rev.* **2014**, *130*, 154–196. [CrossRef]
36. Jolivet, L.; Faccenna, C.; Becker, T.; Tesauro, M.; Sternai, P.; Bouilhol, P. Mantle Flow and Deforming Continents: From India-Asia Convergence to Pacific Subduction. *Tectonics* **2018**, *37*, 2887–2914. [CrossRef] [PubMed]
37. Wang, P.C.; Li, S.Z.; Suo, Y.H.; Guo, L.L.; Santosh, M.; Li, X.Y.; Wang, G.Z.; Jiang, Z.X.; Liu, B.; Zhou, J.; et al. Structural and kinematic analysis of Cenozoic rift basins in South China Sea: A synthesis. *Earth Sci. Rev.* **2021**, *216*, 103522. [CrossRef]
38. Burton-Johnson, A.; Cullen, A.B. Continental rifting in the South China Sea through extension and high heat flow: An extended history. *Gondwana Res.* **2023**, *120*, 235–263. [CrossRef]
39. Li, S.B.; Wang, Y.J.; Wu, S.M. Meso-Cenozoic tectonothermal pattern of the Pearl River Mouth Basin: Constraints from zircon and apatite fission track data. *Earth Sci. Front.* **2018**, *25*, 95–107.
40. Wang, J.L.; Zhang, X.B.; Wu, J.S.; Chen, B.; Zhong, H.Z.; Hao, H.J.; Li, P.L.; Su, N.E. Integrated geophysical researches on base texture of Zhujiang River Mouth Basin. *J. Trop. Oceanogr.* **2002**, *21*, 13–22. (In Chinese with English Abstract)
41. Chen, H.Z.; Wu, X.J.; Zhou, D.; Wang, W.Y.; He, H.J. Meso-Cenozoic faults in Zhujiang River Mouth Basin and their geodynamics background. *J. Trop. Oceanogr.* **2005**, *24*, 52–61. (In Chinese with English Abstract)
42. Sun, Z.; Zhou, D.; Sun, L.T.; Chen, C.M.; Pang, X.; Jiang, J.Q.; Fan, H. Dynamic Analysis on Rifting Stage of Pearl River Mouth Basin through Analogue Modeling. *J. Earth Sci.* **2010**, *21*, 439–454. [CrossRef]
43. Li, P.L. Cenozoic tectonic movement in the Pearl River Mouth Basin. *China Offshore Oil Gas* **1993**, *7*, 11–17. (In Chinese with English Abstract)
44. Cai, Z.R.; Liu, W.L.; Wan, Z.F.; Guo, F. Determination of Cenozoic tectonic movement in the northern South China Sea and the relationship between oil-gas reservoir and tectonic movement. *Mar. Sci. Bull.* **2010**, *29*, 161–165. (In Chinese with English Abstract)
45. Jiang, H.; Wang, H.; Xiao, J.; Chen, S.P.; Lin, Z.L. Control of Paleomorphology to Sedimentary Filling in Marginal Sea Basin—By Taking Zhu III Depression for Example. *J. Oil Gas Technol.* **2008**, *30*, 10–16. (In Chinese with English Abstract)
46. Gong, Y.; Lin, C.S.; Zhang, Z.T.; Zhang, B.; Shu, L.F.; Feng, X.; Hong, F.H.; Xing, Z.C.; Liu, H.Y.; Su, E.Y. Breakup unconformities at the end of the early Oligocene in the Pearl River Mouth Basin, South China Sea: Significance for the evolution of basin dynamics and tectonic geography during rift-drift transition. *Mar. Geophys. Res.* **2019**, *40*, 371–384. [CrossRef]
47. Morley, C.K. Major unconformities/termination of extension events and associated surfaces in the South China Seas: Review and implications for tectonic development. *J. Asian Earth Sci.* **2016**, *120*, 62–86. [CrossRef]
48. Sibuet, J.; Yeh, Y.; Lee, C. Geodynamics of the South China Sea. *Tectonophysics* **2016**, *692*, 98–119. [CrossRef]
49. Niu, Z.C.; Liu, G.D.; Ge, J.W.; Zhang, X.T.; Cao, Z.; Lei, Y.C.; Yuan, A.; Zhang, M.Y. Geochemical characteristics and depositional environment of Paleogene lacustrine source rocks in the Lufeng sag, Pearl River Mouth basin, South China Sea. *J. Asian Earth Sci.* **2018**, *171*, 60–77. [CrossRef]
50. Peng, G.R.; Zhang, X.T.; Xu, X.M.; Bai, H.J.; Cai, G.F.; Zhao, C.; Zhang, Z.W. Important discoveries and understandings of oil and gas exploration in Yangjiang sag of the Pearl River Mouth Basin, northern South China Sea. *China Pet. Explor.* **2019**, *24*, 267–279. (In Chinese with English Abstract)
51. Nanni, U.; Pubellier, M.; Chan, L.S.; Senell, R.J. Rifting and reactivation of a Cretaceous structural belt at the northern margin of the South China Sea. *J. Asian Earth Sci.* **2017**, *136*, 110–123. [CrossRef]
52. Tang, X.; Yu, Y.X.; Zhang, X.T.; Peng, G.R.; Niu, S.L.; Qiu, X.W.; Lu, M.S.; He, Y.B. Multiphase faults activation in the southwest Huizhou Sag, Pearl River Mouth basin: Insights from 3D seismic data. *Mar. Pet. Geol.* **2023**, *152*, 106257. [CrossRef]
53. Li, S.Z.; Cao, X.Z.; Wang, G.Z.; Liu, B.; Li, X.Y.; Suo, Y.H.; Jiang, Z.X.; Guo, L.L.; Zhou, J.; Wang, P.C.; et al. Meso-Cenozoic tectonic evolution and plate reconstruction of the Pacific Plate. *J. Geomech.* **2019**, *25*, 642–677. (In Chinese with English Abstract)

54. Zhan, H.W.; Cai, G.F.; Zhang, Z.W.; Wang, G.Z.; Li, Y.W.; Suo, Y.H.; Wang, P.C.; Jiang, S.H.; Liu, B.; Guo, L.L.; et al. Paleogene fault activity and basin controlling characteristics in the northern South China Sea margin—A case study of the eastern Yangjiang sag. *Geotecton. Metallog.* **2021**, *45*, 20–39. (In Chinese with English Abstract)
55. Li, J.L.; Lei, B.H.; Zheng, Q.G.; Duan, L.; Yan, Y. Stress Field Evolution and its Controls on Oil Accumulation in the Wenchang Sag. *Geotecton. Metallog.* **2015**, *39*, 601–609. (In Chinese with English Abstract)
56. Zhou, J.; Li, S.Z.; Suo, Y.H.; Zhang, L.; Du, X.D.; Cao, X.Z.; Wang, G.Z.; Li, F.K.; Liu, Z.; Liu, J.; et al. NE-Trending transtensional faulting in the Pearl River Mouth basin of the northern South China Sea margin. *Gondwana Res.* **2022**, *120*, 4–19. [CrossRef]
57. Zalán, P.V. Identification of strike-slip faults in seismic sections. In *SEG Technical Program Expanded Abstracts*; Society of Exploration Geophysicists: Houston, TX, USA, 1987; pp. 116–118.
58. Xia, Y.P.; Liu, W.H.; Xu, L.G.; Zheng, L.H. Identification of strike-slip fault and its petroleum geology significance. *Pet. Geol.* **2007**, *1*, 17–23. (In Chinese with English Abstract)
59. Xie, G.J.; Chen, D.X.; Chang, L.; Li, J.H.; Yin, Z.J. Migration and accumulation of crude oils in the Qionghai Uplift, Pearl River Mouth Basin, Offshore South China Sea. *J. Pet. Sci. Eng.* **2021**, *205*, 108943. [CrossRef]
60. Zhao, F.; Alves, T.M.; Xia, S.H.; Li, W.; Wang, L.; Mi, L.J.; Wu, S.G.; Cao, J.H.; Fan, C.Y. Along-strike segmentation of the South China Sea margin imposed by inherited pre-rift basement structures. *Earth Planet. Sci. Lett.* **2020**, *530*, 115862. [CrossRef]
61. He, Z.Y.; Bai, Z.Z.; Wang, W.Y.; Li, L.Z.; Zhang, Y.M.; Chen, Y.; He, T.; Ma, R.Y. Tectonic framework research in Zhujiang River Mouth Basin based on gravity and magnetic data. *Haiyang Xuebao* **2023**, *45*, 25–43. (In Chinese with English Abstract)
62. Xu, J.Y.; Zhang, L.Y. Genesis of Cenozoic basins in northwest Pacific margin (2): Linked dextral pull-apart basin system. *Oil Gas Geol.* **2000**, *21*, 185–190. (In Chinese with English Abstract)
63. Liu, Z.; Li, S.Z.; Suo, Y.H.; Bukhari, S.W.H.; Ding, X.; Zhou, J.; Wang, P.; Cheng, H.; Somerville, I. Evolution of pull-apart basins with overlapping NE-trending strike-slip fault systems in the northern South China Sea margin: Insight from numerical modeling. *Tectonophysics* **2023**, *846*, 229679. [CrossRef]
64. Sun, Z.; Xu, Z.Y.; Sun, L.T.; Pang, X.; Yan, C.Z.; Li, Y.P.; Zhao, Z.X.; Wang, Z.W.; Zhang, C.M. The mechanism of post-rift fault activities in Baiyun sag, Pearl River Mouth basin. *J. Asian Earth Sci.* **2014**, *89*, 76–87. [CrossRef]
65. Cai, G.F.; Zhang, X.T.; Peng, G.R.; Wu, J.; Liu, B.J.; Bai, H.J.; Li, Z.S.; Ma, X.N.; Li, S.Z.; Suo, Y.H. Neogene volcanism and tectonics along the Yangjiang-Yitong'ansha Fault Zone in the Northern South China Sea margin. *Geotecton. Metallog.* **2021**, *45*, 40–52. (In Chinese with English Abstract)
66. Zhang, G.C.; Qu, H.J.; Jia, Q.J.; Zhang, L.G.; Yang, B.; Chen, S.; Ji, M.; Sun, R.; Guan, L.M.; Hayat, K. Passive continental margin segmentation of the marginal seas and its effect on hydrocarbon accumulation: A case study of the northern continental margin in South China Sea. *Mar. Pet. Geol.* **2021**, *123*, 104741. [CrossRef]
67. Hu, Z.W.; Xu, C.G.; Wang, D.Y.; Ren, J.; Liu, Y.F.; Xiao, S.G.; Zhou, X. Superimposed characteristics and genetic mechanism of strike–slip faults in the Bohai Sea, China. *Pet. Explor. Dev.* **2019**, *46*, 254–267. (In Chinese with English Abstract) [CrossRef]
68. Hall, R. Cenozoic geological and plate tectonic evolution of SE Asia and the SW Pacific: Computer-based reconstructions and animations. *J. Asian Earth Sci.* **2002**, *20*, 353–434. [CrossRef]
69. Molnar, P.; Stock, J.M. Slowing of India's convergence with Eurasia since 20 Ma and its implications for Tibetan mantle dynamics. *Tectonics* **2009**, *28*, 1–11. [CrossRef]
70. Copley, A.; Avouac, J.-P.; Royer, J.-Y. India-Asia collision and the Cenozoic slowdown of the Indian plate: Implications for the forces driving plate motions. *J. Geophys. Res. Solid Earth* **2010**, *115*, 1–14. [CrossRef]
71. Li, Y.H.; Zhu, R.W.; Liu, H.L.; Qiu, X.L.; Huang, H.B. The Cenozoic activities of Yangjiang-Yitongdong Fault: Insights from analysis of the tectonic characteristics and evolution processes in western Zhujiang (Pearl) River Mouth Basin. *Acta Oceanol. Sin.* **2019**, *38*, 87–101. [CrossRef]
72. Northrup, C.J.; Royden, L.H.; Burchfiel, B.C. Motion of the Pacific Plate relative to Eurasia and its potential relation to Cenozoic extension along the eastern margin of Eurasia. *Geology* **1995**, *23*, 719–722.
73. Müller, R.D.; Seton, M.; Zahirovic, S.; Williams, S.E.; Cannon, J. Ocean Basin Evolution and Global-Scale Plate Reorganization Events Since Pangea Breakup. *Annu. Rev. Earth Planet. Sci.* **2016**, *44*, 107–138. [CrossRef]
74. Ren, J.Y.; Tamaki, K.; Li, S.T.; Zhang, J.X. Late Mesozoic and Cenozoic rifting and its dynamic setting in Eastern China and adjacent areas. *Tectonophysics* **2002**, *344*, 175–205. [CrossRef]
75. Li, S.Z.; Suo, Y.H.; Li, X.Y.; Wang, Y.M.; Cao, X.Z.; Wang, P.C.; Guo, L.L.; Yu, S.Y.; Lan, H.Y.; Li, S.J.; et al. Mesozoic plate subduction in West Pacific and tectono-magmatic response in the East Asian ocean-continent connection zone. *Chin. Sci. Bull.* **2018**, *63*, 1550–1593. [CrossRef]
76. Ye, Q.; Shi, H.S.; Mei, L.F.; Shu, Y.; Liu, H.L.; Wei, T.; Yan, H. Post-Rift Faulting Migration, Transition and Dynamics in Zhu I Depression, Pearl River Mouth Basin. *Earth Sci.* **2017**, *42*, 105–118. (In Chinese with English Abstract)